Role of *Pneumocystis jirovecii* infection in chronic obstructive pulmonary disease progression in an immunosuppressed rat *Pneumocystis* pneumonia model

TING XUE and CHUN-LI AN

Department of Microbiology and Parasitology, College of Basic Medical Science, China Medical University, Shenyang, Liaoning 110122, P.R. China

Received July 19, 2018; Accepted October 9, 2019

DOI: 10.3892/etm.2020.8545

Abstract. *Pneumocystis jirovecii (P. jirovecii)*, an opportunistic fungal pathogen, is the primary cause of *Pneumocystis* pneumonia (PCP), which affects immunocompromised individuals and leads to high morbidity and mortality. *P. jirovecii* colonization is associated with development of chronic obstructive pulmonary disease (COPD) in patients with HIV infection, and also non-sufferers, and in primate models of HIV infection. However, the mechanisms underlying *P. jirovecii* infection in the pathogenesis of COPD have yet to be fully elucidated. To investigate the pathogenicity of *P. jirovecii* infection and its role in COPD development, the present study established a PCP rat model induced by dexamethasone sodium phosphate injection. Expression of COPD-related biomarkers, including matrix metalloproteinases (MMPs) MMP-2, MMP-8, MMP-9, and MMP-12, and heat shock protein-27 (HSP-27), were quantified in the rat PCP model using reverse transcription-quantitative polymerase chain reaction, ELISA, western blot analysis, immunohistochemistry and gelatin zymography. Body weight, COPD symptoms, and pulmonary histopathology were assessed. Inflammatory cell counts in splenic tissues were measured using flow cytometry. It was identified that MMP and HSP-27 expression increased in the PCP rats, which was in agreement with previous literature. Therefore, it was hypothesized that *P. jirovecii* infection may have an important role in COPD development.

Introduction

Chronic obstructive pulmonary disease (COPD) remains one of the major causes of morbidity and mortality worldwide and is a large global public health burden. Cigarette smoking is the major risk factor for COPD with long-term exposure to cigarette smoke the most common method for establishing COPD in animal models. However, there is increasing attention on the role of infection in the development of COPD, with the opportunistic pathogen *Pneumocystis jirovecii (P. jirovecii)* likely to be a key contributor (1).

Recently, the role of *P. jirovecii* colonization in respiratory diseases has become the focus of research due to a high frequency of *P. jirovecii* colonization among HIV-negative patients, especially those with COPD (2-5). Although the underlying physiopathology remains unclear, results from animal model experiments support the hypothesis that *P. jirovecii* colonization serves a significant role in COPD pathogenesis (6-8). COPD is a chronic inflammatory disorder characterized by airflow limitation, which correlates with a complex inflammatory response in the lungs. *P. jirovecii* colonization leading to infection in the lung tissue can cause pulmonary tissue damage and the deterioration of lung function via inflammation and the related inflammatory mediators. Therefore, *P. jirovecii* colonization affects COPD progression (8).

COPD is accompanied by hypoxia and increased cellular stress in addition to increased inflammation. High expression of matrix metalloproteases (MMPs), including MMP-2, MMP-8, MMP-9, and MMP-12, and chaperone heat shock protein-27 (HSP-27) have been confirmed in both lung tissues of COPD rat models and in COPD patients (9-15). These markers are also closely correlated with COPD development (11,16,17).

The present study aimed to establish a steroid-induced *Pneumocystis* pneumonia (PCP) rat model to study the role of *P. jirovecii* infection in the pathogenesis and development of COPD. Investigation into the expression levels of various COPD-related MMPs and also HSP-27 in PCP rats compared to healthy controls was performed. The present findings provided new insights into the contribution of *Pneumocystis* to COPD pathogenesis and may lead to novel prophylactic treatment options.

Materials and methods

Establishment of a rat PCP model. The protocol for animal experimentation was approved by the Experimental Animal

Correspondence to: Professor Chun-Li An, Department of Microbiology and Parasitology, College of Basic Medical Science, China Medical University, 77 Puhe Road, Shenyang, Liaoning 110122, P.R. China
E-mail: cmucl@126.com

Key words: Pneumocystis pneumonia, chronic obstructive pulmonary disease, matrix metalloproteinases, heat shock protein-27, pathogenesis

Care and Ethics Committee of China Medical University. A total of 20 female Wistar rats (mean weight, 150±20 g; age, 5-7 weeks) were purchased from the Department of Experimental Animal Center, China Medical University. Rats were randomly divided into two groups: A control group and a PCP group with ten rats per group. All rats were housed in a temperature (20-25˚C) and humidity (53-58%)-controlled facility with a 12-h light/dark cycle with food and water provided *ad libitum*. The antibiotic oxytetracycline (1 g/l; Yichuang Pharmaceutical Co., Ltd.) was added to the drinking water to prevent bacterial infections. The immune response of the PCP group rats was suppressed by intraperitoneal dexamethasone sodium phosphate injections (3 mg per rat; Rongsheng Pharmaceutical Co., Ltd) twice per week, for 8 successive weeks. The control group was injected with physiological saline. The rats were weighed once a week. Fur color and thickness, activity, breathing, death rate, and other symptoms and signs of respiratory distress were monitored throughout the study.

Processing of lung tissue specimens. After 8 weeks, rats were weighed, anesthetized with an intraperitoneal injection of sodium pentobarbital (50 mg/kg) then sacrificed by rapid exsanguination. Blood was collected via the abdominal aorta and serum was isolated for detection of MMPs and HSP-27. The lower lobe of the right lung was fixed for further histopathological assessment. The middle lobe of the right lung was removed for preparation of lung imprint smears. After ligation of the right lung, bronchoalveolar lavage (BAL) was performed in the left lung. All remaining lung tissue was frozen and stored in liquid nitrogen for further use.

Pathogen identification. The presence of *P. jirovecii* organisms was confirmed by Giemsa and Gomori's methenamine silver nitrate staining assays (GMS) of the lung imprint smears from the cross-sections of the middle lobe of the right lungs, according to a previously described protocol (18).

Histopathological examination. Two-thirds of the lower lobe of the right lung were fixed with 4% paraformaldehyde (Dingguo Biotechnology Co. Ltd.) at room temperature for >24 h. The lung tissue sections were then washed, dehydrated, embedded in paraffin and sectioned at 5 μm thick preparations. The sections were placed onto glass slides, dewaxed, dehydrated and stained with hematoxylin (5 min) and eosin (for 3-5 min) (HE) at room temperature or subsequently used for immunohistochemical staining. Histological changes in the lung tissues were respectively observed under a light microscope (Magnifications, x200 and x400; Olympus Coporation).

Flow cytometry. A direct immunofluorescence staining method was used. Homogenates made from splenic tissues were collected and passed through a screen mesh (pores size, 70 μm; cat. no. 258368; Wuxi NEST Biotechnology Co., Ltd.). Antibodies were added after lysis of red blood cells (at 4˚C for 4-5 min) and adjustment of cell concentrations ($1x10^6$ cells/ml). Pre-cooled PBS (cat no. FG701-01; Beijing Transgen Biotech Co., Ltd.) was used to terminate the lysis reaction at 4˚C. T lymphocytes were stained with PerCP-anti-CD8 (0.2 mg/ml; cat. no. 558824; BD Biosciences) and BV421-anti-CD4 (0.2 mg/ml, cat no: 740040, BD Biosciences). M1 macrophages were stained with PE-Anti-CD86 (0.2 mg/ml; cat no: 551396, BD Biosciences) and granulocytes with fluorescein isothiocyanate-anti-granulocytes (0.5 mg/ml, cat no: 554907, BD Biosciences). BD Pharmingen™ Stain Buffer (FBS; cat no. 554656; BD Biosciences) was applied as the washing reagent. Corresponding isotype-matched monoclonal antibodies were used as negative controls. All antibodies used in flow cytometry were purchased from BD Biosciences. Inflammatory cell counts were analyzed using BD FACSDiva™ Software (version 6.2; BD Biosciences) combined with a BD LSRFortessa™ flow cytometer (BD Biosciences).

ELISA. Expression levels of MMPs and HSP-27 in the bronchoalveolar lavage fluid (BALF) and serum were quantified using the following ELISA kits (Cusabio Biotech Co., Ltd.): MMP-2 ELISA kit (cat. no. CSB-E07411r); Rat MMP8 (neutrophil collagenase) ELISA kit (cat. no. CSB-E07406r); Rat MMP-9 (Gelatinase B) ELISA Kit (cat. no. CSB-E08008r); Rat MMP12 (Macrophage metalloelastase) ELISA kit (cat. no. CSB-EL014659RA); and Rat heat shock protein 27 (HSP-27) ELISA Kit (cat. no. CSB-E09240r) according to the manufacturer's protocols. In brief, standards and samples (100 μl) were added to appropriate wells and incubated for 2 h at 37˚C. The liquid was removed from all wells, and 100 μl of biotin-antibody (1X) were added to each well, and incubated for 1 h at 37˚C. The residual liquid in all wells was removed and the microtiter plate was washed three times with wash buffer (200 μl) using a multi-channel pipette for 2 min per wash. Then, 100 μl of horseradish peroxidase-avidin (1X) was added to each well and incubated for 1 h at 37˚C. The aspiration/wash process was repeated five times. Then, 90 μl of the 2,2'5,5'-Tetramethylbenzidine substrate were added to each well and incubated for 15-30 min at 37˚C. The chromogenic reaction was terminated with the addition of 50 μl stop solution. Optical density at 450 nm wavelength was determined immediately using a Thermo Scientific Varioskan® Flash (Thermo Fisher Scientific, Inc.).

Immunohistochemical detection. Immunohistochemical detection of MMPs and HSP-27 in lung tissue was performed using the Streptavidin-Peroxidase (SP) method and the UltraSensitive™ SP IHC kit (cat. no. Kit-9720; Fuzhou Maixin Biotech Co., Ltd.) according to the manufacturer's protocols. Two-thirds of the lower lobe of the right lung were fixed with 4% paraformaldehyde (Beijing Dingguo Changsheng Biotechnology Co., Ltd.) at room temperature for >24 h. The lung tissue was then washed, dehydrated, embedded in paraffin and sectioned into 5-μm thick preparations. Antigen retrieval was performed in sodium citrate buffer (pH 6.0) at 100˚C for 1 min followed by cooling at room temperature for 1 min, a process which was repeated a further three times. After blocking for 30 min at 37˚C with goat serum (included in the UltraSensitive SP IHC kit), slices were incubated with primary antibodies against MMP-2 (1:250; cat. no. ab37150; Abcam), MMP-8 (1:250; cat. no. ab81286; Abcam), MMP-9 (1:250; cat. no. ab76003; Abcam), MMP-12 (1:250; cat. no. ab52897; Abcam), and HSP-27 (1:250; cat. no. ab5579; Abcam) overnight at 4˚C. After washing with PBS three times, a horseradish peroxidase-conjugated secondary antibody (included

Table I. Primer sequences used for reverse transcription-quantitative polymerase chain reaction.

Primer	Sequence (5'-3')	Product size (bp)
MMP-2 forward	GTGGCAATGGAGATGGACAG	127
MMP-2 reverse	CGGTCATAATCCTCGGTGGT	
MMP-8 forward	CAGTGCCTCCAGAACACCTG	120
MMP-8 reverse	CGGCAATCATAGTGGCATTC	
MMP-9 forward	GTGACACCGCTCACCTTCAC	122
MMP-9 reverse	GCGTGTGCCAGTAGACCATC	
MMP-12 forward	CGATGTGGAGTGCCTGATGT	113
MMP-12 reverse	GCACGCTTCATGTCTGGAGT	
HSP-27 forward	CAACTCAGCAGCGGTGTCTC	115
HSP-27 reverse	CCACGCCTTCCTTGGTCTTA	
GAPDH forward	GACATGCCGCCTGGAGAAAC	92
GAPDH reverse	AGCCCAGGATGCCCTTTAGT	

MMP, matrix metalloprotease; HSP, heat shock protein.

in the UltraSensitive SP IHC kit) was added to samples and incubated for 30 min at 37˚C. PBS was used as a negative control. The DAB detection kit (Fuzhou Maixin Biotech, Co., Ltd.) was applied to visualize the distribution and location of MMPs and HSP-27 expression. Brown staining indicated positive protein detection. Five regions of positive expression on each slide were selected randomly and photographed under light microscopy (Olympus Corporation). Integrated optical density (IOD) was analyzed by Image pro plus 6.0 (Media Cybernetics, Inc.).

Reverse transcription-quantitative polymerase chain reaction (RT-qPCR). Total RNA was extracted from lung tissue using RNAiso Plus (Takara Bio, Inc.). RNA concentration was quantified using a NanoDrop™ 2000 (Thermo Fisher Scientific, Inc.) and samples were diluted to 1 μg of RNA. Reverse transcription was performed with a PrimeScript™ RT reagent kit with gDNA Eraser (Takara Bio, Inc.) according to manufacturer's protocols. qPCR was subsequently performed using the ABI 7500 real-time PCR instrument (Thermo Fisher Scientific, Inc.) with TB Green™ Premix Ex Taq™ II (Tli RNaseH Plus; Takara Bio, Inc) in 20 μl reaction mixtures. The thermocycling conditions for qPCR amplification were as follows: Initial denaturation at 95˚C for 30 sec, followed by 40 cycles of 95˚C for 5 sec and 60˚C for 34 sec. All primers used in the present study and their sequences are listed in Table I. Data were analyzed using the $2^{-\Delta\Delta Cq}$ method (19). GAPDH was used as housekeeping gene for normalizing the levels of MMPs and HSP-27 mRNA.

Western blot analysis. Protein was extracted from the lung tissues using the ProteinExt® Mammalian Total Protein Extraction Kit (cat no. DE101-01; Beijing TransGen Biotech Co., Ltd.) and quantified using the Bicinchonininc protein assay kit (Beijing Dingguo Changsheng Biotechnology Co., Ltd.). Protein samples were separated using gel electrophoresis (Bio-Rad Laboratories, Inc.) by SDS-PAGE on a 10% gel. The proteins were transferred to a polyvinylidene difluoride membrane. Blocking was performed with 5% bovine serum albumin (BSA; Beijing Solarbio Science & Technology Co., Ltd.). in Tris-buffered saline with 0.05% Tween-20 (TBST) for 2 h at room temperature. The membranes were incubated with the following primary antibodies diluted in 5% BSA TBST: Anti-MMP-2 (1:2,000; cat. no. ab37150; Abcam), anti-MMP-8 (1:2,000; cat. no. ab81286; Abcam), anti-MMP-9 (1:2,000; cat. no. ab76003; Abcam), anti-MMP-12 (1:2,000; cat. no. ab52897; Abcam) and anti-HSP-27 (1:1,000; cat. no. ab5579; Abcam) then incubated overnight at 4˚C. Following 10 min washes three times, the membranes were incubated with goat anti-Rabbit IgG (cat. no. ZB-2301) and goat anti-Mouse IgG (cat. no. ZB-2305) secondary antibodies conjugated to horseradish peroxidase (both 1:5,000; Beijing Zhongshan Jinqiao Biotechnology Co. Ltd.; OriGene Technologies, Inc.) for 2 h at room temperature. Following the second washing step (six times for 5 min each), membranes were visualized with SuperSignal West Pico PLUS Chemiluminescent Substrate, an enhanced chemiluminescent (ECL) reagent (Thermo Fisher Scientific, Inc.) and analyzed using the Tanon-5200 automatic chemiluminescence imaging analysis system. GAPDH was used to normalize the relative density of each protein band in each group. The intensity of the protein bands was analyzed with Image J software (version 1.8.0; National Institutes of Health).

Gelatin zymography. The prepared protein samples were separated by 10% SDS-PAGE containing 1% w/v gelatin by gel electrophoresis (Bio-Rad Laboratories, Inc.) at 4˚C. The gelatin zymography assay kit (Wanlei Biotech Co., Ltd) was used to detect MMP-2 and MMP-9 activity. The gel was subsequently washed four times in eluate for 15 min per wash, washed with rinse buffer twice for 20 min each, and then incubated in incubation buffer for 48 h at 37˚C. After staining with Coomassie Brilliant Blue R-250 for 3 h, incubation with decolorized buffer was performed at room temperature for 2 h resulting in the appearance of white bands on a blue background.

Statistical analysis. All statistical analyses were performed using the statistical software SPSS 13.0 (SPSS Inc.) and results were presented using Prism 7 (GraphPad Software, Inc.). All values were expressed as mean ± standard deviation. The means of two groups were compared using the Student's t test after testing for normality and homogeneity of variance. $P<0.05$ was considered to indicate statistical significance.

Results

Clinical features and gross findings. Compared with the control, rats in the PCP group had decreased body weight after 4 weeks (Fig. 1), and their fur density was reduced and fur color was darker. PCP rats displayed decreased activity and always herded in the corner of the cage. PCP rats also occasionally displayed wheezing.

Pathogenic identification. *Pneumocystis* cysts, identified as brown or brown-reddish spheres or ovoids with a small black stick-shape figure in the middle, were visualized using GMS staining (Fig. 2A). On Giemsa stained lung imprint smears, cyst walls were not stained and thus formed transparent zones. Every cyst contained 2-8 blue-stained intracystic bodies that were arranged in the shape of a ring (Fig. 2B). Typical *Pneumocystis* cysts assumed a crescent or irregular spherical shape. No signs of *Pneumocystis* cysts were observed in the control group (data not shown).

Lung appearance. Shrinkage of lung volume and hardening of the lung tissue was observed in the PCP group (Fig. 3). Gray or white dots were interspersed on the surface of the lung tissue in PCP rats. No serious gross pulmonary lesions, such as hemorrhage or necrosis, were observed in the PCP group. None of the rats died during steroid treatment.

PCP induces histopathological changes in rat lungs. Histopathologic examination was performed under light microscopy at magnifications of x200 and x400. Morphologically, lung sections of rats in the control group were free of cellular infiltrate and mucus, and did not show any pathological abnormality. The structure of the lung interstitial tissue was intact and the alveolar space was clear (Fig. 4A). The degree of histopathological changes varied in lungs of the PCP rats. The inflammatory cell infiltrate in the pulmonary interstitial tissue primarily included lymphocytes and macrophages (Fig. 4B). Diffuse pulmonary interstitial tissue hyperplasia and interstitial edema was observed (Fig. 4C). Lesions in the form of red foamy alveolar exudates (Fig. 4D) and consolidated areas in lung tissue (Fig. 4E) were identified. Morphological signs of emphysema, including alveolar fusion in the sectional tissue and pulmonary bullae due to alveolar wall destruction were also present.

PCP increases inflammatory cell counts. Flow cytometry analysis determined that compared with the control group, the numbers of $CD8^+$ T lymphocytes ($P<0.01$; Fig. 5), M1 macrophages ($P<0.01$; Fig. 5), and granulocytes ($P<0.01$; Fig. 5) were significantly increased in the splenic tissue of PCP rats, whilst the number of $CD4^+$ T lymphocytes was significantly reduced ($P<0.01$; Fig. 5).

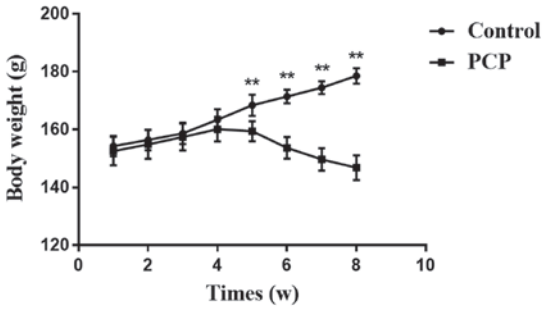

Figure 1. Comparison of body weights between the control and PCP groups. After 4 weeks rats in the PCP group exhibited reduced body weight compared with the control group. **P<0.01 vs. Control. PCP, *Pneumocystis* pneumonia.

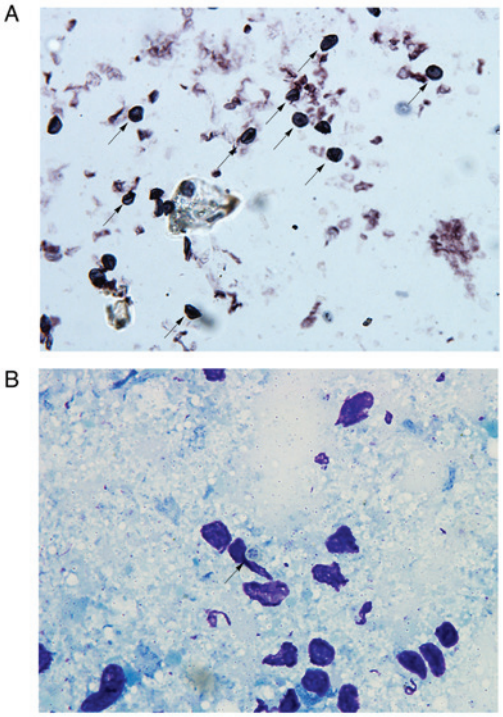

Figure 2. Pathogenic identification by GMS and Giemsa staining. (A) GMS staining. *Pneumocystis* cysts were identified as brown/brown-reddish spheres or ovoids with a black small stick-shape figure in the middle (indicated by arrows). (B) Giemsa staining. *Pneumocystis* cyst walls were not stained and thus formed transparent zones. Every cyst contained 2-8 blue-stained intracystic bodies that were arranged in the shape of a ring (indicated by arrow). GMS, Gomori's methenamine silver nitrate.

PCP increases MMPs and HSP-27 secreted levels in serum and BALF. The concentrations of MMPs and HSP-27 in rat serum and BALF were determined by ELISA (Fig. 6). MMPs and HSP-27 expression levels in the serum and BALF were significantly higher in the PCP group compared with the control group.

PCP increases MMPs and HSP-27 protein expression in pulmonary tissue. Positive protein expression was detected by brown staining upon immunohistochemical analysis. HSP-27 expression was largely located in the bronchial epithelial cells and a few other cell types in the PCP group (Fig. 7). Positive MMP expression was clearly detected in the cytoplasm and nuclei of cells in the PCP group, particularly in macrophages

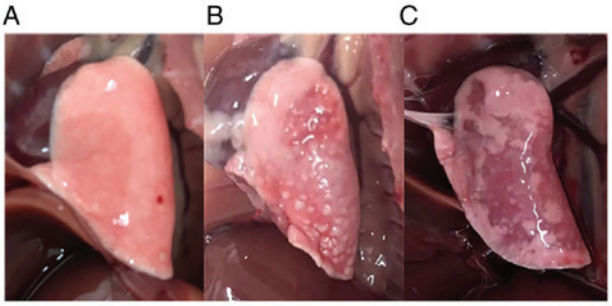

Figure 3. Gross appearance of lung tissue. (A) The control group lung tissue appeared soft and light pale pink and maintained a smooth, flat surface without lesions. (B and C) The lung tissue was dark red and hard with a rough surface in the PCP group. Gray or white dots were interspersed on the surface of the lung tissue in the PCP rats. Viscous liquid oozed out when the lesions were extruded. Marked pulmonary congestion and tissue edema of lung tissue in the PCP group were observed. No serious gross pulmonary lesions, such as hemorrhage or necrosis, were observed. PCP, *Pneumocystis* pneumonia.

and alveolar epithelial cells (Fig. 7). However, there was weak or no staining for MMPs and HSP-27 in the control group. In the PCP model group, positive expression was demonstrated by darker staining (Fig. 7). The IOD values of MMPs and HSP-27 were significantly higher in the PCP group compared to the control group ($P<0.01$; Fig. 8).

PCP increases MMP and HSP-27 mRNA and protein expression levels in lung tissue. RT-qPCR and western blot results demonstrated that MMPs and HSP-27 mRNA and protein expression levels in the lung tissues were significantly upregulated in the PCP group compared to the control group ($P<0.01$; Figs. 9 and 10). Gelatin zymography revealed that there was higher activity of MMP-9 and MMP-2 in the PCP model group compared to the control group (Fig. 11).

Discussion

The underlying pathological processes leading to the development of COPD remain unclear at present however several studies have demonstrated that colonization of pathogenic microorganisms in the tracheobronchial tree could serve as inflammatory stimuli in the airways of stable COPD patients and possibly lead to disease progression (20). Recurrent acute infections are strongly correlated with the occurrence of acute exacerbation of COPD (21). The lungs of patients with COPD become susceptible to airway mucosal infections by pathogenic microorganisms. Morris *et al* (1,8) demonstrated that an increase in *P. jirovecii* colonization in COPD is independently correlated with the degree of airway obstruction. PCP is a serious complication that can lead to death for patients infected with HIV. Compared with HIV negative patients, lung function of COPD patients infected with HIV rapidly declines. Acute PCP has been associated with obstructive pulmonary changes (7). The present study investigated the pathogenicity of *Pneumocystis* infection and its role in the progression of COPD using an immunosuppressed rat PCP model to determine the expression of COPD-related cytokine expression and inflammatory cell populations.

Advances in research of *P. jirovecii* pathogenicity have been limited by the difficulties in cultivating *P. jirovecii in vitro*

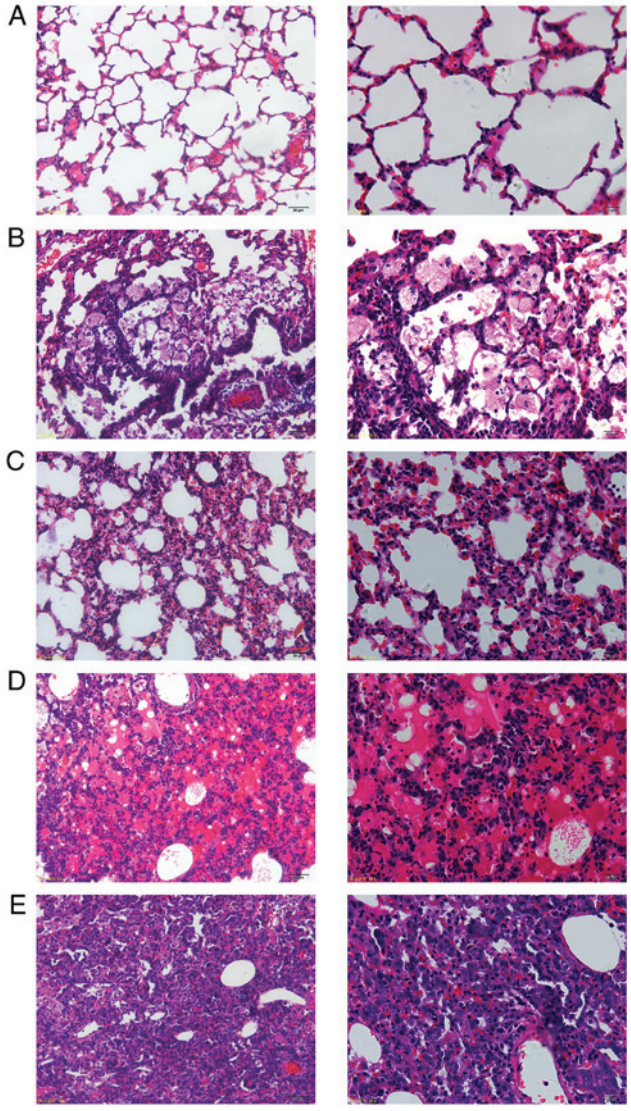

Figure 4. Histopathological examination using hematoxylin and eosin staining. Histopathologic changes were observed under light microscopy at magnifications of x200 (left panels) and x400 (right panels). (A) Normal lung tissue. (B) Inflammatory cell infiltration into pulmonary tissue in the PCP model group. (C) Diffuse pulmonary interstitial tissue hyperplasia and interstitial edema in pulmonary tissue in the PCP model group. (D) Red foamy alveolar exudates. (E) Consolidated areas in lung tissue in the PCP model group. PCP, *Pneumocystis* pneumonia.

for an extended time period. Therefore, *in vitro Pneumocystis* studies are scarce. For *in vivo* studies of *Pneumocystis*, rats are the most commonly used animal model. Immunosuppressed rats induced by steroids can be spontaneously infected with *P. jirovecii*, resulting in pathologic features closely resembling PCP in humans (22-24).

The present study demonstrated that various degrees of pulmonary pathology appeared in steroid-induced PCP model rats. Gross clinical changes included body weight loss, fur density and color changes, decreased activity level, and respiratory symptoms. Histopathological changes included inflammatory cell infiltration, diffuse lung interstitial tissue hyperplasia, and appearance of consolidation areas. Similar histopathological changes have been described previously in cigarette smoke-induced COPD model rats (25). Morris *et al* (1,7,8) reported that the frequency of fibrous

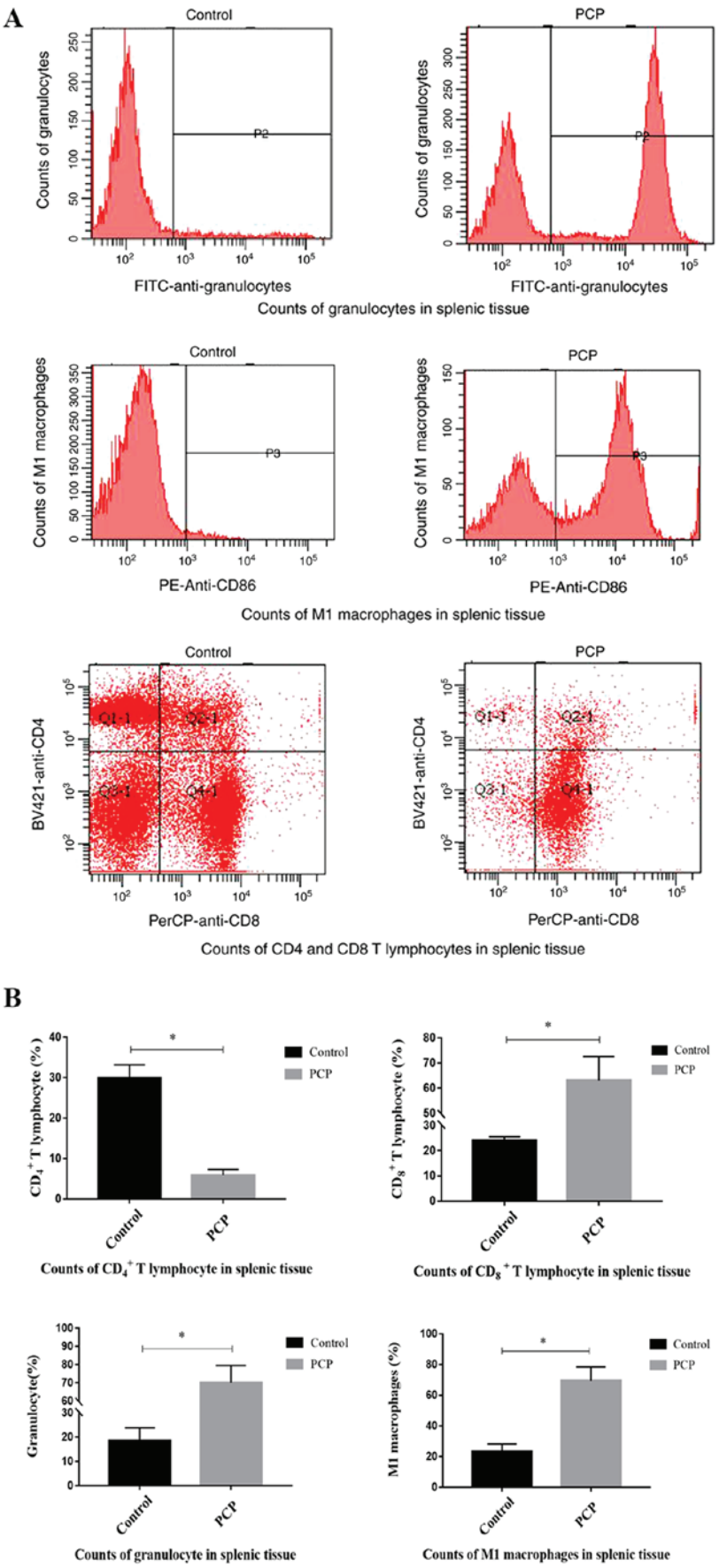

Figure 5. PCP increases inflammatory cell counts determined by flow cytometry. (A) T lymphocytes were stained with PerCP-anti-CD8 and BV421-anti-CD4. M1 macrophages were stained with PE-Anti-CD86 and granulocytes with FITC-anti-granulocytes. Counts of macrophages, lymphocytes, and granulocytes in splenic tissues from the control and PCP groups were analyzed by flow cytometry. (B) The quantitative analysis of the inflammatory cell counts for CD4+ T lymphocytes, CD8+ T lymphocytes, M1 macrophages and granulocytes. *P<0.01. PCP, *Pneumocystis* pneumonia; CD, cluster of differentiation; FITC, fluorescein isothiocyanate; PE, phycoerythrin.

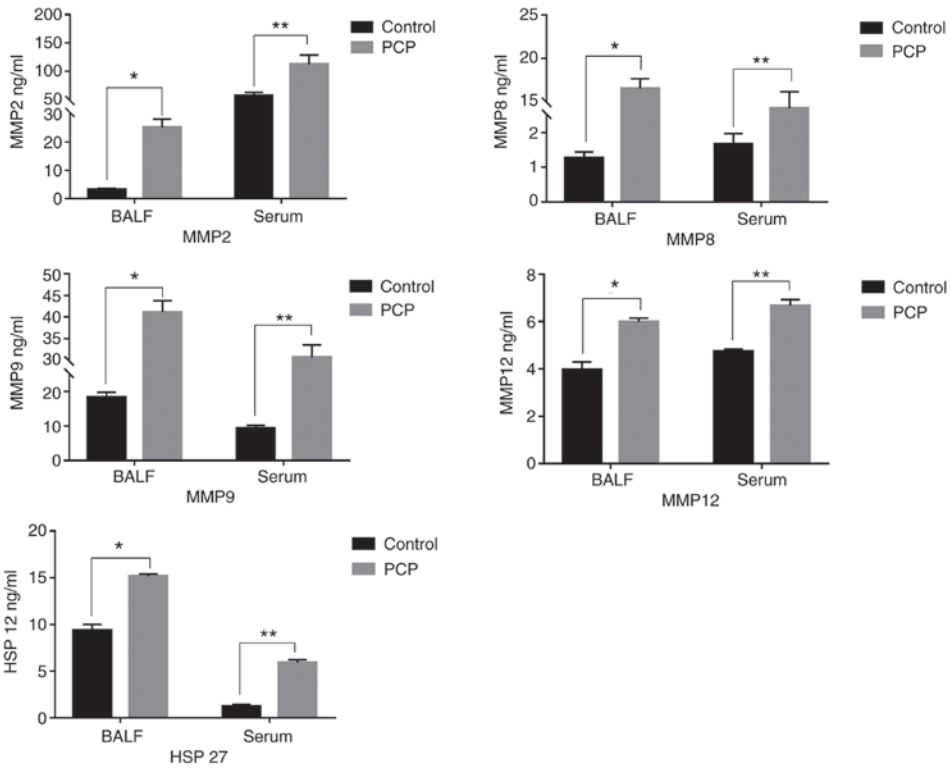

Figure 6. PCP increases inflammatory protein levels in BALF and serum. Concentrations of MMPs and HSP-27 in rat serum and BALF detected using ELISA assays. *P<0.05 and **P<0.01 vs. control. PCP, *Pneumocystis* pneumonia; BALF, bronchoalveolar lavage fluid; MMP, matrix metalloprotease; HSP, heat shock protein.

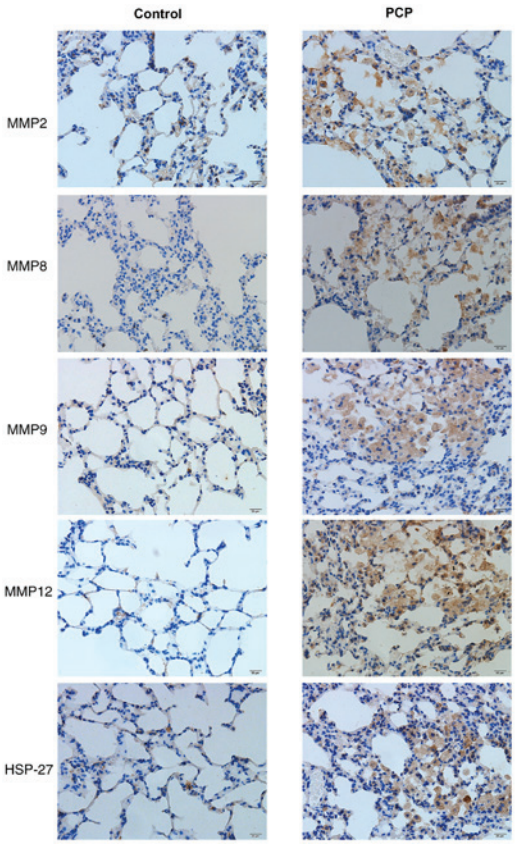

Figure 7. PCP increases MMP and HSP-27 protein expression in pulmonary tissue. Immunohistochemical analysis for MMP2, MMP8, MMP9, MMP12 and HSP-27 expression in lung tissues of control and PCP groups. Positive protein staining appears brown, while nuclear staining appears blue. Magnification, x400. PCP, *Pneumocystis* pneumonia; MMP, matrix metalloprotease; HSP, heat shock protein.

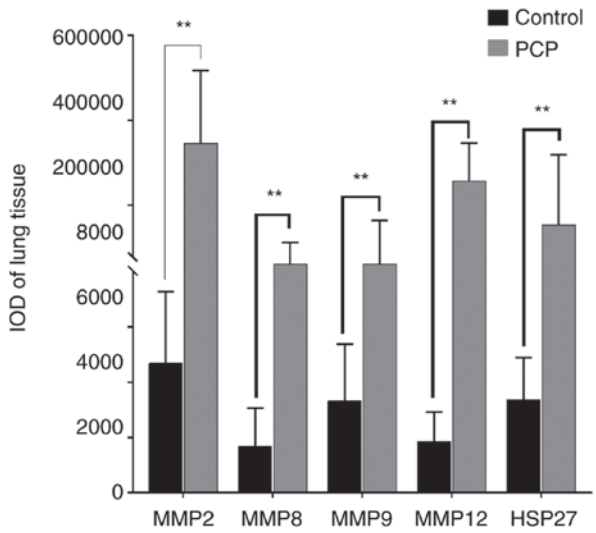

Figure 8. PCP significantly increases MMP and HSP-27 levels in pulmonary tissue. IOD values from the immunohistochemistry staining for MMP2, MMP8, MMP9, MMP12 and HSP-27. **P<0.01 vs. control. PCP, *Pneumocystis* pneumonia; MMP, matrix metalloprotease; HSP, heat shock protein. IOD, integrated optical values.

degeneration in lung tissue and obstructive pathological changes were higher in patients with PCP compared with patients without PCP. Consequently, animal and human studies investigating the changes of pulmonary pathology support the hypothesis that *P. jirovecii* infection has an important role in COPD progression.

The present study determined that there was a close correlation between the immune response and severity of

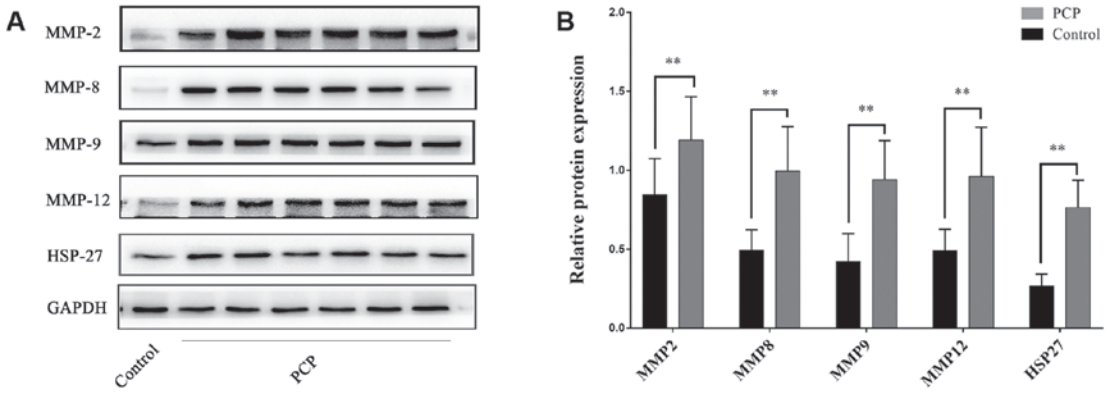

Figure 9. PCP increases MMP and HSP-27 protein expression levels in lung tissue. (A) Representative western blots. (B) Quantification of protein expression levels relative to GAPDH. **P<0.01 vs. control. PCP, *Pneumocystis* pneumonia; MMP, matrix metalloprotease; HSP, heat shock protein.

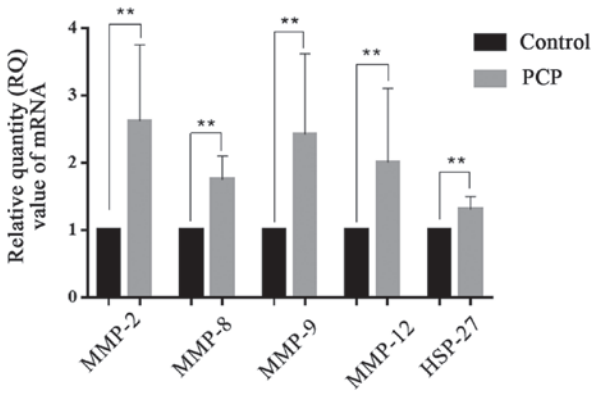

Figure 10. PCP increases MMP and HSP-27 mRNA expression levels in lung tissue. Relative band densities of MMP and HSP-27 mRNA expression levels relative to GAPDH, using reverse transcription-quantitative polymerase chain reaction. **P<0.01 vs. control. PCP, *Pneumocystis* pneumonia; MMP, matrix metalloprotease; HSP, heat shock protein; RQ, relative quantity.

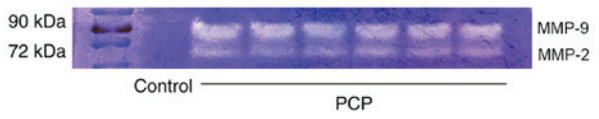

Figure 11. Representative images of MMP-2 and MMP-9 activity by gelatin zymography. MMP, matrix metalloprotease; PCP, *Pneumocystis* pneumonia.

pulmonary impairment. The severity of pathological lesions increased with declining levels of $CD4^+$ T lymphocytes and increasing levels of $CD8^+$ T lymphocytes, M1 macrophages, and granulocytes. Lung tissue may be damaged directly by the inflammatory responses of organisms. It has been previously demonstrated that $CD8^+$ T lymphocytes serve a significant role in the pathogenic process of PCP (26). Similar inflammatory cell count results were reported in rat studies of cigarette-smoke-induced COPD (27-29). COPD is a chronic inflammatory disorder characterized by irreversible airflow limitation, which correlates with a complex inflammatory response in the lungs. $CD8^+$ T lymphocytes, M1 macrophages, and granulocytes cause pathological injury to the pulmonary airway, blood vessels, and lung tissue which decreases pulmonary function, and leads to chronic inflammation and COPD pathogenesis. Importantly, COPD patients with higher GOLD (The Global Initiative for Chronic Obstructive Lung Disease) stages demonstrate a more severe inflammatory response (30-32).

At present, there are various theories concerning the mechanism of COPD (33) with an imbalance in protease-antiprotease one of the most widely accepted. MMPs, neutrophil elastase, serine protease, and other proteases are regarded to be the key drivers. MMPs are mainly secreted and produced by alveolar macrophages, neutrophils, and lung structural cells. Basement membrane and extracellular matrix (ECM) are degraded by MMPs, which contributes to progressive destructive inflammation in the airway and pulmonary tissue leading to COPD development. MMPs are also the principal inflammatory mediators of emphysema and have a regulatory role in the inflammatory process. Elevated levels of MMPs have been detected in COPD patients, particularly in the patients with exacerbated COPD (12,13,25,34). MMP-2 and MMP-9 are released into the intercellular space in the form of inactive zymogens. Following activation, they have pivotal roles in proteolysis. The present study demonstrated by western blot analysis that MMP-2, MMP-8, MMP-9 and MMP-12 expression levels were upregulated in PCP model rats compared with control rats. In addition, gelatin zymography assay revealed that MMP-2 and MMP-9 activity was increased in PCP model rats. Therefore, it was hypothesized that *P. jirovecii* infection may lead to the release of endogenous proteases which is in accordance with the literature (6,35-37). In addition, upregulated levels of MMPs suggested that the occurrence and progression of emphysema may be caused by *P. jirovecii* colonization due to release of endogenous proteases and stimulation of protease release in the lung tissue of PCP model rats which is in agreement with a previous study (38) Similar upregulation of MMP levels have also been previously reported in COPD rats (33). Findings suggested that ECM degradation caused by a protease-antiprotease imbalance due to *P. jirovecii* infection may have an important role in COPD progression.

HSP-27, an important small heat shock protein, is a COPD biomarker. HSP-27 levels increase during oxidative stress, hypoxia, and inflammation. Among these stressors, oxidative responses of macrophages represent an important component of microbicidal effector cell function against a variety of potential pathogens (39). The phagocytosis of pathogens mediated by macrophages has been correlated with the release

of oxygen radicals (40). Previous studies have confirmed that *Pneumocystis* is associated with the induction of oxidative stresses in alveolar macrophages (41,42). The present study determined that HSP-27 expression was higher in the PCP model group compared with the control group, which suggested that *P. jirovecii* infection was involved in inducing an oxidative burst in alveolar macrophages. Upregulated levels of HSP-27 have also been identified in COPD smokers compared with non-COPD smokers (16,17,43,44). Elevated HSP-27 expression indicates that *P. jirovecii* infections may serve a role in COPD progression.

The complex mechanisms of COPD remain unclear however cigarette smoking and pathogenic infection are currently regarded as the two major risk factors. Christensen *et al* (38) demonstrated that cigarette smoke exposure can increase the pulmonary *Pneumocystis* burden whilst *Pneumocystis* and cigarette smoke exposure can cause airspace enlargement. A limitation of the present study was that the causal relationship between *P. jirovecii* colonization or infection and COPD was not definitively established. The interaction between cigarette smoke exposure and *Pneumocystis* may synergistically speed up the progression of COPD. Further confirmation of the role of *Pneumocystis* infections in the progression of COPD and the causal relationship between these are crucial for understanding the pathogenesis of COPD and for the development of novel prophylactic treatment options.

In conclusion, the present study established a rat model of PCP via steroid injection, and then tested the pathogenicity of *P. jirovecii* infection, investigated the inflammatory response following PCP, and evaluated the expression of factors closely related to COPD, including MMPs and HSP-27. The present findings suggested that *Pneumocystis* caused pulmonary inflammation similar to COPD, which may contribute to lung tissue destruction, as well as the development of pulmonary emphysema, protease-antiprotease imbalance, and induction of oxidative stress in alveolar macrophages. It was demonstrated that *P. jirovecii* infection may have an indirect role in the progression of COPD therefore providing evidence for *Pneumocystis* pathogenicity and its role in COPD development and progression.

Acknowledgements

Not applicable.

Funding

The current study was supported by the Natural Science Foundation of China (grant no. 81370189).

Availability of data and materials

The datasets used and/or analyzed during the current study are available from the corresponding author on reasonable request.

Authors' contributions

The current study was designed and conceived by TX and CLA, and performed and analyzed by TX. Data acquisition, statistical analysis, and manuscript preparation were performed by TX. CLA reviewed and edited the manuscript. All authors contributed to the drafting and revision of the paper, as well as data analysis. All authors read and approved the final manuscript and are responsible for all aspects of this study.

Ethics approval and consent to participate

The protocol for animal experimentation was approved by the Experimental Animal Care and Ethics Committee of China Medical University (Liaoning, China).

Patient consent for publication

Not applicable.

Competing interests

The authors declare that they have no competing interests.

References

1. Morris A and Norris KA: Colonization by Pneumocystis jirovecii and its role in disease. Clin Microbiol Rev 25: 297-317, 2012.
2. Wang DD, Zheng MQ, Zhang N and An CL: Investigation of Pneumocystis jirovecii colonization in patients with chronic pulmonary diseases in the People's Republic of China. Int J Chron Obstruct Pulmon Dis 10: 2079-2085, 2015.
3. Gutiérrez S, Respaldiza N, Campano E, Martinez-Risquez MT, Calderón EJ and De La Horra C: Pneumocystis jirovecii colonization in chronic pulmonary disease. Parasite 18: 121-126, 2011.
4. Khodavaisy S, Mortaz E, Mohammadi F, Aliyali M, Fakhim H and Badali H: Pneumocystis jirovecii colonization in Chronic Obstructive Pulmonary Disease (COPD). Curr Med Mycol 1: 42-48, 2015.
5. Martínez Lamas L, Pérez Rodríguez MT, Álvarez Ramos I, Bouza Soage ME, Figueroa Lamas MP and Álvarez Fernández M: Role of Pneumocystis jirovecii in patients with different pulmonary underlying condition using a nested-PCR. Rev Esp Quimioter 31: 336-343, 2018.
6. Kling HM, Shipley TW, Patil SP, Kristoff J, Bryan M, Montelaro RC, Morris A and Norris KA: Relationship of Pneumocystis jiroveci humoral immunity to prevention of colonization and chronic obstructive pulmonary disease in a primate model of HIV infection. Infect Immun 78: 4320-4330, 2010.
7. Morris A, Sciurba FC, Lebedeva IP, Githaiga A, Elliott WM, Hogg JC, Huang L and Norris KA: Association of chronic obstructive pulmonary disease severity and Pneumocystis colonization. Am J Respir Crit Care Med 170: 408-413, 2004.
8. Morris A, Sciurba FC and Norris KA: Pneumocystis: A novel pathogen in chronic obstructive pulmonary disease? COPD 5: 43-51, 2008.
9. Ankersmit HJ, Lambers C, Zimmermann M, Hacker S and Moser B: Serendipity and technical considerations for the measurement of serum heat shock protein HSP27 in patients with COPD and lung cancer. Cell Stress Chaperones 20: 727-728, 2015.
10. Chen W, Cui X, Xing J and Wu T: Response to: Hsp27 and Hsp70 in chronic obstructive pulmonary disease. Cell Stress Chaperones 20: 725-726, 2015.
11. Ünver R, Deveci F, Kirkil G, Telo S, Kaman D and Kuluöztürk M: Serum heat shock protein levels and the relationship of heat shock proteins with various parameters in chronic obstructive pulmonary disease patients. Turk Thorac J 17: 153-159, 2016.
12. Cane JL, Mallia-Millanes B, Forrester DL, Knox AJ, Bolton CE and Johnson SR: Matrix metalloproteinases -8 and -9 in the airways, blood and urine during exacerbations of COPD. COPD 13: 26-34, 2016.
13. Koo HK, Hong Y, Lim MN, Yim JJ and Kim WJ: Relationship between plasma matrix metalloproteinase levels, pulmonary function, bronchodilator response, and emphysema severity. Int J Chron Obstruct Pulmon Dis 11: 1129-1137, 2016.

14. Sng JJ, Prazakova S, Thomas PS and Herbert C: MMP-8, MMP-9 and neutrophil elastase in peripheral blood and exhaled breath condensate in COPD. COPD 14: 238-244, 2017.
15. Esquivel AL, Pérez-Ramos J, Cisneros J, Herrera I, Rivera-Rosales R, Montaño M and Ramos C: The effect of obesity and tobacco smoke exposure on inflammatory mediators and matrix metalloproteinases in rat model. Toxicol Mech Methods 24: 633-643, 2014.
16. Jan Ankersmit H, Nickl S, Hoeltl E, Toepker M, Lambers C, Mitterbauer A, Kortuem B, Zimmermann M, Moser B, Bekos C, *et al*: Increased serum levels of HSP27 as a marker for incipient chronic obstructive pulmonary disease in young smokers. Respiration 83: 391-399, 2012.
17. Hu R, Ouyang Q, Dai A, Tan S, Xiao Z and Tang C: Heat shock protein 27 and cyclophilin A associate with the pathogenesis of COPD. Respirology 16: 983-993, 2011.
18. An CL, Li S, Jiang L and Masanobu T: Detection of the Pneumocystis carinii by PCR and organism staining method. J China Med Univ 28: 27-28, 1999 (In Chinese).
19. Livak KJ and Schmittgen TD: Analysis of relative gene expression data using real-time quantitative PCR and the 2(-Delta Delta C(T)) method. Methods 25: 402-408, 2001.
20. Sethi S, Maloney J, Grove L, Wrona C and Berenson CS: Airway inflammation and bronchial bacterial colonization in chronic obstructive pulmonary disease. Am J Respir Crit Care Med 173: 991-998, 2006.
21. Sethi S: Infection as a comorbidity of COPD. Eur Respir J 35: 1209-1215, 2010.
22. Fan H, Guo JY, Ma SL, Zhang N and An CL: Synthetic p55 tandem DNA vaccine against Pneumocystis carinii in rats. Microbiol Immunol 60: 397-406, 2016.
23. Feng Y, Guo S, Jiang T, Han X, Liu P, Wu T and Luo Y: Active immunization against Pneumocystis carinii with p55-v3 DNA vaccine in rats. Can J Microbiol 57: 375-381, 2011.
24. Liu AB, Pu Y, Zheng YQ, Cai H and Ye B: Therapeutic efficacies of chitosan against Pneumocystis pneumonia of immunosuppressed rat. Parasite Immunol 36: 292-302, 2014.
25. Sun J, Bao J, Shi Y, Zhang B, Yuan L, Li J, Zhang L, Sun M, Zhang L and Sun W: Effect of simvastatin on MMPs and TIMPs in cigarette smoke-induced rat COPD model. Int J Chron Obstruct Pulmon Dis 12: 717-724, 2017.
26. An CL, Su XP and Harmsen AG: The role of CD8+ T cells in the pathogenesis of Pneumocystis carinii pneumonia in mice depleted of CD4+ T cells. Zhongguo Ji Sheng Chong Xue Yu Ji Sheng Chong Bing Za Zhi 18: 207-212, 2000.
27. Eppert BL, Wortham BW, Flury JL and Borchers MT: Functional characterization of T cell populations in a mouse model of chronic obstructive pulmonary disease. J Immunol 190: 1331-1340, 2013.
28. Jiang SL, Li Y, Tian YG, Li JS, Li SY, Wang Y, Wang YY and Deng L: Influence and long-term effects of three methods for regulating and invigorating fei-shen on T lymphocyte subsets and CD4+ CD25+ in COPD rats. Zhongguo Zhong Xi Yi Jie He Za Zhi 33: 1538-1544, 2013 (In Chinese).
29. Zhu X, Gadgil AS, Givelber R, George MP, Stoner MW, Sciurba FC and Duncan SR: Peripheral T cell functions correlate with the severity of chronic obstructive pulmonary disease. J Immunol 182: 3270-3277, 2009.
30. Cazzola M, Page CP, Calzetta L and Matera MG: Emerging anti-inflammatory strategies for COPD. Eur Respir J 40: 724-741, 2012.
31. Chung KF and Adcock IM: Multifaceted mechanisms in COPD: Inflammation, immunity, and tissue repair and destruction. Eur Respir J 31: 1334-1356, 2008.
32. Thatcher TH, Hsiao HM, Pinner E, Laudon M, Pollock SJ, Sime PJ and Phipps RP: Neu-164 and Neu-107, two novel antioxidant and anti-myeloperoxidase compounds, inhibit acute cigarette smoke-induced lung inflammation. Am J Physiol Lung Cell Mol Physiol 305: L165-L174, 2013.
33. Mocchegiani E, Giacconi R and Costarelli L: Metalloproteases/anti-metalloproteases imbalance in chronic obstructive pulmonary disease: Genetic factors and treatment implications. Curr Opin Pulm Med 17 (Suppl 1): S11-S19, 2011.
34. Vlahos R, Bozinovski S, Chan SP, Ivanov S, Lindén A, Hamilton JA and Anderson GP: Neutralizing granulocyte/macrophage colony-stimulating factor inhibits cigarette smoke-induced lung inflammation. Am J Respir Crit Care Med 182: 34-40, 2010.
35. Qu J, Rong Z, He L, Pan J and Chen X: Relationship between the burden of Pneumocystis carinii, the inflammatory reaction and lung injury in Pneumocystis carinii pneumonia. Chin Med J (Engl) 113: 1071-1074, 2000.
36. Sukura A, Konttinen YT, Sepper R, Kaartinen L, Sorsa T and Lindberg LA: Collagenases and the serine proteinases elastase and cathepsin G in steroid-induced Pneumocystis carinii pneumonia. J Clin Microbiol 33: 829-834, 1995.
37. Norris KA, Morris A, Patil S and Fernandes E: Pneumocystis colonization, airway inflammation, and pulmonary function decline in acquired immunodeficiency syndrome. Immunol Res 36: 175-187, 2006.
38. Christensen PJ, Preston AM, Ling T, Du M, Fields WB, Curtis JL and Beck JM: Pneumocystis murina infection and cigarette smoke exposure interact to cause increased organism burden, development of airspace enlargement, and pulmonary inflammation in mice. Infect Immun 76: 3481-3490, 2008.
39. Sibille Y and Reynolds HY: Macrophages and polymorphonuclear neutrophils in lung defense and injury. Am Rev Respir Dis 141: 471-501, 1990.
40. Johnston RB Jr, Godzik CA and Cohn ZA: Increased superoxide anion production by immunologically activated and chemically elicited macrophages. J Exp Med 148: 115-127, 1978.
41. Pesanti EL: Interaction of cytokines and alveolar cells with Pneumocystis carinii in vitro. J Infect Dis 163: 611-616, 1991.
42. Hidalgo HA, Helmke RJ, German VF and Mangos JA: Pneumocystis carinii induces an oxidative burst in alveolar macrophages. Infect Immun 60: 1-7, 1992.
43. Hacker S, Lambers C, Hoetzenecker K, Pollreisz A, Aigner C, Lichtenauer M, Mangold A, Niederpold T, Zimmermann M, Taghavi S, *et al*: Elevated HSP27, HSP70 and HSP90 alpha in chronic obstructive pulmonary disease: Markers for immune activation and tissue destruction. Clin Lab 55: 31-40, 2009.
44. Kelsen SG, Duan X, Ji R, Perez O, Liu C and Merali S: Cigarette smoke induces an unfolded protein response in the human lung: A proteomic approach. Am J Respir Cell Mol Biol 38: 541-550, 2008.